J|A|C|S
ARTICLES
Published on Web 03/21/2006

Stochastic Modeling of CW-ESR Spectroscopy of [60]Fulleropyrrolidine Bisadducts with Nitroxide Probes

Antonino Polimeno,* Mirco Zerbetto, Lorenzo Franco, Michele Maggini, and Carlo Corvaja*

Contribution from the Dipartimento di Scienze Chimiche - Università degli Studi di Padova, Via Marzolo 1, 35131 Padova, Italy

Received October 31, 2005; E-mail: antonino.polimeno@unipd.it; carlo.corvaja@unipd.it

Abstract: In this work, we address the interpretation of continuous wave electron spin resonance (CW-ESR) spectra of fulleropyrrolidine bisadducts with nitroxide addends. Our approach is based on a definition of the spin Hamiltonian which includes exchange and dipolar interactions and on a complete numerical solution of the resulting stochastic Liouville equation, with inclusion of diffusive rotational dynamics. CW-ESR spectra are simulated for a series of C_{60} bisadducts made up of four trans isomers and the equatorial isomer. A nonlinear least-squares fitting procedure allows extraction directly from the available experimental spectra of a wide range of parameters, namely interprobe relative distances, diffusion tensors, and values of the exchange parameter *J*. Results are in good agreement with previous, more phenomenological estimates, proving that the combination of sensitive ESR spectroscopy based on multiple spin labeling with nitroxide radicals and sophisticated modeling can be highly helpful in providing structural and dynamic information on molecular systems.

I. Introduction

Interpretation of structural and dynamic behavior of complex molecular systems, with particular accent on biological macromolecules, is of fundamental importance to understand their stability, chemical functions and activities, and catalytic action. For instance, physicochemical properties of proteins depend, ultimately, on the synergetic action of different motions at several time and length scales,[1,2] and information on multiscale dynamics in proteins can be gained, in principle, by a variety of spectroscopic techniques, magnetic[3] (nuclear magnetic resonance, NMR, electron spin resonance, ESR, electron nuclear double resonance, ENDOR) and optic[4−6] (fluorescence polarization anisotropy, FPA, dynamic light scattering, DLS, time-resolved Stokes shift, TRSS).

Nitroxide free radicals probes and spin labels are employed extensively to obtain information from ESR spectra on structural and dynamic properties of biomolecules, micelles, and membranes.[7] In particular, measurements performed on proteins via site directed spin labeling (SDSL) are highly informative. Nitroxide derivatives are linked directly to substituted cysteine residues in the protein, allowing, in principle, detection of several data at once: secondary structure information from the motion of lateral chains,[8] large amplitude protein motions from the overall ESR spectrum shape,[9,10] and inter-residual distances.[11]

The wealth of structural and dynamic information which can be extracted from CW-ESR, pulsed ESR or ENDOR spectra in SDSL is, at present, limited experimentally by the difficulty of obtaining extensive multifrequency data on spin-labeled proteins and theoretically by the necessity of employing computationally efficient dynamic models. The latter problem can be tackled, at least in principle, by a numerical approach based on the direct solution of the stochastic Liouville equation (SLE) describing the density matrix of the system in the presence of relaxation processes. Notwithstanding the relative complexity of the SLE-based approach, it can be said that it constitutes a valid tool for interpreting sensitive ESR information in complex molecular environments. In the past, several applications and examples have been presented which are related to SLE-based interpretation of ESR spectroscopy in liquid and liquid crystalline phases,[12,13] and applications to biological systems are starting to appear in the literature.[14]

Most of the available studies are concentrated on mononitroxide derivatives, although biradicals and polyradicals have been used in the past for liquid crystals and membranes studies[15]

(1) Ishima, R.; Torchia, D. A. *Nat. Struct. Biol.* **2000**, *7*, 740.
(2) Atkinson, R. A.; Kieffer, B. *Prog. Nucl. Magn. Reson. Spectrosc.* **2004**, *44*, 141.
(3) Freed, J. H. In *Biological Magnetic Resonance*; Eaton, S. S., Eaton, G. R., Berliner, L. J., Eds.; Kluwer/Plenum Press: New York, 2005; Vol. 24, pp 239−268.
(4) Barone, F.; Matzeu, M.; Mazzei, F.; Pedone, F. *Biophys. Chem.* **1999**, *78*, 259.
(5) Soglie, S. S.; Pecora, R. *Macromolecules* **1988**, *21*, 1437.
(6) Brauns, E. B.; Madaras, M. L.; Coleman, R. S.; Murphy, C. J. *J. Am. Chem. Soc.* **1999**, *121*, 11644.
(7) Mottley, C.; Mason, R. P. In *Biological Magnetic Resonance*; Berliner, L. J., Reuben, J., Eds.; Plenum Press: New York, 1989; Vol. 8, pp 489−546.
(8) Klug, C. S.; Feix, J. B. In *Biological Magnetic Resonance*; Eaton, S. S., Eaton, G. R., Berliner, L. J., Eds.; Kluwer/Plenum Press: New York, 2005; Vol. 24, pp 269−308.
(9) Hubbell, W. L.; Mchaourab, H. S.; Altenbach, C.; Lietzow, M. A. *Structure* **1996**, *4*, 779.
(10) Steinhoff, H. J. *Frontiers Biosci.* **2002**, *7*, 97.
(11) Eaton, S. S., Eaton, G. R., Berliner, L. J., Eds; *Biological Magnetic Resonance*; Kluwer/Plenum Press: New York, 2000; Vol. 19.
(12) Meirovitch, E.; Igner, D.; Igner, D.; Moro, G.; Freed, J. H. *J. Chem. Phys.* **1982**, *77*, 3915.
(13) Polimeno, A.; Freed, J. H. *J. Phys. Chem.* **1995**, *99*, 10995.
(14) Liang, Z.; Lou, Y.; Freed, J. H.; Columbus, L.; Hubbell, W. L. *J. Phys. Chem. B* **2004**, *108*, 17649.

10.1021/ja057414i CCC: $33.50

and are being employed as spin labels in biopolymer and peptide model systems.[16] Nitroxide biradicals are characterized by anisotropic tensor **g** and ^{14}N hyperfine coupling tensor **A** like monoradicals, but contain additional interaction terms in the spin Hamiltonian, namely the exchange interaction and the dipolar interaction between the unpaired electrons. The distance between the radicals is inferred from the measurement of the dipolar interaction,[11] but structural information can be gained also from measuring the exchange constant *J* between radicals. Conformations of macromolecules have been studied in this way.[17]

Measurements of the exchange interaction are somewhat difficult to interpret, because of the lack of knowledge of its dependence on relative *distance and orientation* of the radicals. Theoretical calculations have been conducted to evaluate the exchange interaction in different molecular geometries,[18,19] which however can hardly be tested by comparison with controlled experimental findings, given the difficulty of preparing binitroxide model systems with defined relative distances and orientations in rigid molecular structures.

As a rigid template, C_{60} has been shown to be an ideal candidate to support nitroxide groups placed at fixed distances and orientations. An ESR study was recently presented[20] for a series of C_{60} bisadducts, which provides a good example of a geometrically controlled molecular system where the relative position of the unpaired electron couple is exactly determined. As such, it is amenable to an advanced theoretical modeling, which includes explicitly the molecular rotational dynamics based on the SLE formalism, employed extensively for the interpretation of ESR spectra of monoradicals.[21]

In this work we propose to apply the standard SLE approach to interpret experimental ESR observables for this series of bisadducts, elucidating the formal aspects and summarizing the necessary computational steps, with an emphasis on the general strategy more than on the technical details. The paper is organized as follows. In the next section we recall briefly the molecular structure of the bisadducts under investigation, and we present the SLE and the computational approach employed to calculate ESR spectra. Results are presented in section III. Conclusions are outlined in section IV.

II. Molecular System and Modeling

The series of biradicals studied in ref 20 are C_{60} bisadducts containing the C_{2v} symmetric tetramethylpyrrolidine-1-oxyl group. The bisadducts series include all four *trans*-isomers **1**−**4** and the equatorial isomer **5**, and they are shown in Figure 1. Notice that for isomers **1**−**4** the exchange magnitude, *J*, is of the same order of magnitude of the hyperfine coupling; the measured ESR spectra are complex and show the presence of several transitions. A description of the synthetic procedures, together with ESR sample preparation and magnetic resonance measurements are provided in ref 20.

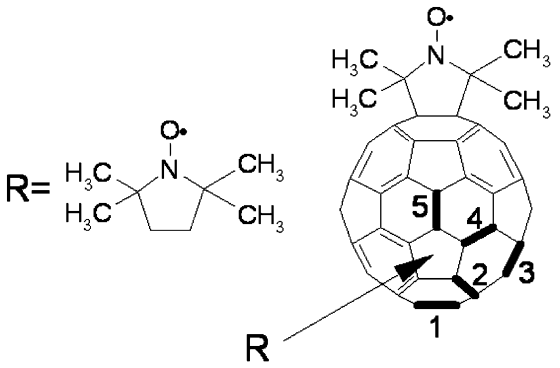

Figure 1. Structures of biradicals **1**−**4** (trans isomers) and **5** (equatorial isomer).

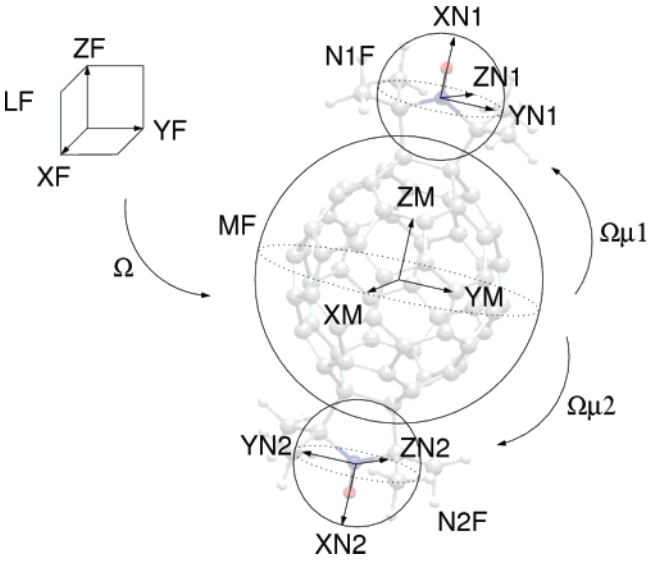

Figure 2. Reference frames employed in the stochastic Liouville equation.

II.A. Modeling. We start by defining the magnetic Hamiltonian of the system which includes Zeeman, hyperfine exchange, and dipolar interaction for the two nitroxides labeled **1** and **2**

$$\hat{H} = \frac{\beta_e}{\hbar}\sum_i \vec{B}_0 \cdot \mathbf{g}_i \cdot \hat{S}_i + \gamma_e \sum_i \hat{I}_i \cdot \mathbf{A}_i \cdot \hat{S}_i - 2\gamma_e J \hat{S}_1 \cdot \hat{S}_2 + \frac{\mu_0}{4\pi}\frac{g_e^2\beta_e^2}{\hbar r^3}\left[\hat{S}_1 \cdot \hat{S}_2 - \frac{3}{r^2}(\hat{S}_1 \cdot \vec{r})(\hat{S}_2 \cdot \vec{r})\right] \quad (1)$$

where the first term is the Zeeman interaction of each electron spin with magnetic field $\vec{B}_0$, depending on the $\mathbf{g}_i$ tensor; the second term is the hyperfine interaction of each coupled ^{14}N/unpaired electron, defined with respect to hyperfine tensor $\mathbf{A}_i$; the third and fourth term represent the exchange and dipolar term, respectively. Here, tensors $\mathbf{g}_i$, $\mathbf{A}_i$ are diagonal in the local frame N_iF rigidly fixed on the *i*th nitroxide (we assume here for simplicity that both tensors are diagonal in the same local frame); operators $\hat{I}_i$, $\hat{S}_i$ are defined in the laboratory or inertial frame (LF); finally $\vec{r}$ is the distance between the two nitroxides. The system geometry is summarized in Figure 2. The set of Euler angles Ω defines the relative orientation of the generic

(15) (a) Luckhurst, G. R. In *Spin Labeling, Theory and Applications*; Berliner, L. J., Ed.; Academic Press: New York, 1976; pp 133−181. (b) Meier, P.; Blume, A.; Ohmes, E.; Neugebauer, F. A.; Kothe, G. *Biochemistry* **1982**, *21*, 526.
(16) Miick, S. M.; Martinez, G. V.; Fiori, W. R.; Todd, A. P.; Millhauser, G. L. *Nature* **1992**, *359*, 653.
(17) (a) Millhauser, G. L. *Biochemistry* **1995**, *34*, 3873. (b) Millhauser, G. L. *Biochemistry* **1995**, *34*, 10318.
(18) Toniolo, C.; Valente, E.; Formaggio, F.; Crisma, M.; Pilloni, G.; Corvaja, C.; Toffoletti, A.; Martinez, G. V.; Hanson, M. P.; Millhauser, G. L.; George, C..; Flippen-Anderson, J. L. *J. Pept. Sci.* **1995**, *1*, 45.
(19) Hanson, P.; Millhauser, G. L.; Formaggio, F.; Crisma, M.; Toniolo, C. *J. Am. Chem. Soc.* **1996**, *118*, 7618.
(20) Mazzoni, M.; Franco, L.; Corvaja, C.; Zordan, G.; Menna, E.; Scorrano, G.; Maggini, M. *ChemPhysChem* **2002**, *6*, 527.
(21) Schneider, D. J.; Freed, J. H. *Adv. Chem. Phys.* **1989**, *73*, 487.

molecular frame (MF), fixed rigidly on the fullerene backbone, with respect to the LF; the local frames N_iF are in turn defined with respect to MF by a set of angles Ω_i. Each nitroxide is finally identified by a set of polar coordinates $\vec{r}_i = (r_i,\varphi_i,\vartheta_i)$, where we take the center of the fullerene backbone as the origin and we assume that the center of the N−O bond represents the nitroxide effective position, and $\vec{r} = \vec{r}_1 - \vec{r}_2$. The Hamiltonian in eq 1 can be also written in the compact form

$$\hat{H} = \frac{\beta_e}{\hbar}\sum_i \vec{B}_0 \cdot \mathbf{g}_i \cdot \hat{S}_i + \gamma_e \sum_i \hat{I}_i \cdot \mathbf{A}_i \cdot \hat{S}_i + \hat{S}_1 \cdot \mathbf{T} \cdot \hat{S}_2 \tag{2}$$

$$\mathbf{T} = \left(-2\gamma_e J + \frac{\mu_0}{4\pi}\frac{g_e^2\beta_e^2}{\hbar r^3}\right)\mathbf{1} - \frac{\mu_0}{4\pi}\frac{g_e^2\beta_e^2}{\hbar r^5}\begin{pmatrix} r_x^2 & r_x r_y & r_x r_z \\ r_x r_y & r_y^2 & r_y r_z \\ r_x r_z & r_y r_z & r_z^2 \end{pmatrix}$$

where **T** is the interaction tensor summarizing both exchange and dipolar interaction. Following the standard approach of description of ESR signals in liquids, we define the SLE

$$\frac{\partial \rho(Q,t)}{\partial t} = -i[\hat{H}(Q),\rho(Q,t)] - \hat{\Gamma}(Q)\rho(Q,t) = -[i\hat{H}^{\times}(Q) + \hat{\Gamma}(Q)]\rho(Q,t) = -\hat{\mathcal{L}}(Q)\rho(Q,t) \tag{3}$$

describing the time evolution of the density matrix of the system, depending upon general stochastic coordinates Q, controlled by the stochastic operator $\hat{\Gamma}$. Here $\hat{H}^{\times}$ is the quantum Liouville operator, i.e., the commutator superoperator defined with respect to $\hat{H}$.[13] In general several relaxation processes can be invoked, corresponding to different fast and slow degrees of freedom subject to Brownian motions and described by many-body Fokker−Planck operators. Here we adopt the simplest choice of considering as only relevant variables the orientation of MF in the LF, i.e., the Euler angles set, $Q = \Omega$. We shall also assume that the system reorients freely in space, subject to a simple diffusive motional regime, i.e.

$$\hat{\Gamma} = D_x\hat{J}_x^2 + D_y\hat{J}_y^2 + D_z\hat{J}_z^2 \tag{4}$$

where $\hat{J}_i$ is the ith component of the angular momentum operator in the molecular frame.

The ESR spectrum is obtained as the Fourier−Laplace transform of the correlation function for the x-component of the magnetization, defined as $|v\rangle = (2I+1)^{-1}(|\hat{S}_{x,1}\rangle + |\hat{S}_{x,2}\rangle)$, where I is the nuclear spin. Following standard definitions[21] we obtain

$$G(\omega - \omega_0) = \frac{1}{\pi}\mathrm{Re}\{\langle v|[i(\omega-\omega_0) + (i\hat{H}^{\times} + \hat{\Gamma})]^{-1}|vP_{eq}\rangle\} \tag{5}$$

where $P_{eq} = 1/8\pi^2$ is the (isotropic) distribution in the Ω space. Here, ω is the sweep frequency, and $\omega_0 = g_0\beta_e B_0/\hbar = \gamma_e B_0$, and g_0 is the trace of each $\mathbf{g}_i$ tensor, which is the same for the two electrons. The starting vector $|v\rangle$, with respect to which the resolvent in eq 5 is evaluated, is related to the allowed ESR transitions, and it is actually an operator acting on the electron spin degrees of freedom.[13]

To summarize, a bisadduct is described as a diffusive rotator, bearing two spin probes rigidly fixed. Parameters are (1) the principal values of the diffusion tensor, D_x, D_y, D_z; (2) the principal values of the **g** and **A** tensors and Euler angles Ω_i, specifying the orientation of magnetic local tensors with respect to MF, and finally (3) the exchange interaction J.

II.B. Computational Treatment. We present here in qualitative form the general computational procedure, for the sake of completeness. A reader not interested in the details of the numerical implementation can safely skip this part and go directly to the Results section.

The computational implementation of eq 5 is accomplished by converting the problem to a standard linear algebraic formulation of the resolvent in terms of matrices/vectors by projecting the Liouvillean $\hat{\mathcal{L}}$ and the starting vector $|v\rangle$ on a suitable basis set that, in our case, can be initially defined as

$$|\sum\rangle = |p_1^S q_1^S p_1^I q_1^I\rangle \otimes |p_2^S q_2^S p_2^I q_2^I\rangle \otimes |LMK\rangle = |\sigma_1,\sigma_2,LMK\rangle \tag{6}$$

where the same notation of ref 21 is used; the basis set is given by the direct product of spin operators of nitroxide 1 and 2, defined by electron and nuclear spin quantum numbers p_i^S, q_i^S, p_i^I, q_i^I,[13,21] globally indicated as σ_i, and of normalized Wigner rotation matrices $|LMK\rangle$, which correspond to the rotational degrees of freedom, with $L > 0$, $-L \le M,K \le L$. It is convenient to introduce a symmetrized basis set, which allows exploiting symmetry properties of the Liouville operator[21]

$$|\sum\rangle_K = |\sigma_1,\sigma_2,j^K LMK\rangle = [2(1+\delta_{K,0})]^{-1/2} e^{-i\pi(j^K-1)/4}[|+\rangle + j^K s^K|-\rangle] \tag{7}$$

where $s^K = (-1)^{L+K}$, with $K \ge 0$, and $j^K = \pm 1$ for $K > 0$, $(-1)^L$ for $K = 0$; ket symbols $|+\rangle$, $|-\rangle$ stand for $|\Sigma\rangle$ and $|\Sigma\rangle$- with $K \rightarrow -K$. Matrix elements of the stochastic Liouvillean in the symmetrized basis set are real. A symmetric matrix representation of the Liouville operator is given as:

$$\langle\sum_1|\hat{\mathcal{L}}|\sum_2\rangle_K = \frac{1}{2}[(1+\delta_{K,0})(1+\delta_{K',0})]^{-1/2} \times [\delta_{jK1,jK2}\,\mathrm{Re}\{\langle+|\hat{\mathcal{L}}|+\rangle + j^{K_2}s^{K_2}\langle+|\hat{\mathcal{L}}|-\rangle\} + \delta_{jK1,-jK2}\,\mathrm{Im}\{\langle+|\hat{\mathcal{L}}|+\rangle + j^{K_2}s^{K_2}\langle+|\hat{\mathcal{L}}|-\rangle\}] \tag{8}$$

The basis set has 12 indexes, leading to very large matrices that need to be treated to evaluate each spectrum. Fortunately, a number of established techniques profitably exploited in the past for the study of many-body stochastic Liouville and Fokker−Planck operators can be employed to reduce the computational burden. Exact procedures to reduce the basis dimension invoking rotational symmetries and approximate techniques, based on pruning schemes of the complete basis set, can be employed. First, however, to evaluate explicitly symmetrized or unsymmetrized matrix elements, one needs to make explicit the dependence of the super Hamiltonian $i\hat{H}^{\times}$ from magnetic and orientational parameters. Following the established route used for monoradicals[13,21] we adopt a spherical irreducible tensorial representation

$$\hat{H}^{\times} = \sum_{\mu}\sum_{l=0,2}\sum_{m,m'=-l}^{l} D^l_{mm'}(\Omega)F^{(l,m')}_{\mu,MF} * \hat{A}^{(l,m)}_{\mu,LF} \tag{9}$$

where μ runs over all possible interactions, $D^l_{mm'}(\Omega)$ is a generic Wigner matrix, $F^{(l,m')*}_{\mu,MF}$ is build from elements of $\mathbf{g}_i$,$\mathbf{A}_i$,**T**

in the MF, $\hat{A}^{(l,m)}_{\mu,LF}$ is obtained from spin operators. Next the Liouvillean matrix elements are straightforwardly calculated in the unsymmetrized basis set, and the symmetrized matrix is built. The starting vector is also easily calculated, since $\langle\Sigma|v\rangle_K \propto \delta_{j^K,1}\langle\Sigma|v\rangle$. Explicit matrix element in the unsymmetrized set are obtained following standard arguments reported elsewhere.[13,21] Finally, eq 5 can be converted in matrix/vector and standard algorithms for tridiagonalization, and direct evaluation of spectral densities in continuous fraction form can be employed, like Lanczos or conjugate gradient.[21] The basis set dimension is given by the product of the number of possible magnetic transition for each spin (electrons and nuclei) and the number of normalized Wigner rotation matrices up to a given truncation value L_{max}. In our case, with two electrons and two ^{14}N nuclei, the total number of magnetic basis functions is $4 \times 4 \times 9 \times 9 = 1296$, while for a given L_{max} the number of Wigner functions is given by the sum $\sum_{l=0}^{L_{max}} (2l+1)^2$; for instance, for $L_{max} = 2$, which has been employed throughout this work, the number of rotational basis functions is 35, leading to a basis set dimension of 45360.

These are the typical dimensions of matrices that need to be employed for evaluating the ESR spectrum. Albeit relatively large, this is not a prohibitive dimension. On a desktop Pentium IV PC, a C program based on the Lanczos algorithm is able to calculate a spectrum, for a given set of parameters, in less than 15 min. Furthermore, it is possible to reduce significantly the computational burden by selecting relevant basis set elements, adopting the so-called *pruning* scheme which has been extensively used by Freed and co-workers for monoradicals. Details on the pruning scheme are given elsewhere,[22] and we give here, for sake of completeness, just a general description. The pruning scheme is based on the conjugate gradient algorithm, and it looks at the spectrum, at a given frequency, as obtained in the form $G(\omega) = \langle v|u(\omega)\rangle$; the vector $|u(\omega)\rangle$ is found solving, via conjugate gradient algorithm, a linear system of equations. Basis elements can be classified in term of their projection on $|u(\omega)\rangle$. Sampling the spectrum in a representative range of frequencies, one can find a reduced basis set made only of elements whose projection is higher than that of a given tolerance. Our extensive tests have shown that, even adopting rather conservative criteria in determining the relevant basis element based on the pruning scheme, in the system studied here we are often left with an effective dimension less than 10−20% of the original one, without any significant loss of accuracy in the spectrum evaluation. This fact allows us to determine accurately and quickly the overall spectrum (less than 30 s per spectrum), and thus, a systematic fitting procedure of parameters becomes feasible.

III. Results

The following fitting strategy has been adopted. Principal values of the magnetic tensors have been chosen in accordance with previous knowledge;[23] for both nitroxides we have therefore $g_x = 2.009$, $g_y = 2.006$, $g_z = 2.003$, and $A_x = 5.0$, $A_y = 5.0$, $A_z = 34.5$ G. Geometry has been also chosen according to molecular structure of each isomer. Finally, the following dissipative and magnetic parameters have been left freely changing, and therefore determined via a least-squares fitting of simulated spectra to experimental data: the principal values of the diffusion tensor D_x, D_y, D_z and the exchange coupling constant J. As far as geometrical parameters are concerned, Euler angle set Ω_i specifying the relative orientation of the magnetic tensors, i.e., local frames N_iF, with respect to MF have been inferred from molecular geometry, as shown in Figure 1. Similarly, both spin probes and polar angles ϑ_i,φ_i have been estimated from the conformer geometry. Fitting has been employed explicitly instead, only to determine the effective value of the distance from center for the two nitroxides, $r_1 = r_2 = R$.

A well-established search algorithm based on the Levenberg−Marquardt approach has been employed.[21]

III.A. Fitting Multicomponents. However, a preliminary analysis has shown that in all cases the experimental spectra could not be fit to a single component, i.e., a single simulated ESR result. Essentially, in all cases the intensity of the hyperfine components corresponding to $I_{z,1} \neq I_{z,2}$ were shown to be rather overemphasized in the simulated spectra. By accepting as a working hypothesis that the molecules are essentially rigid objects, without additional degrees of freedom such as fast local libration of the nitroxide residues, we have attempted to add to the simulated one a second component corresponding to a monoradical, which is calculated with standard SLE.[21] For the monoradical the same diffusion tensor of the biradical was assumed:

$$G(\omega) = (1-p)G_{mono}(\omega) + pG_{bi}(\omega) \qquad (10)$$

The additional parameter p was considered free to change. Although the analytical data for **1**−**5** are fully in agreement with the proposed structures, we cannot exclude the presence, in the samples of the bisadducts, of traces of a monoradical species. The synthesis of binitroxides **1**−**5** is in fact based on the oxidation, with chloroperbenzoic acid, of the corresponding bisamines,[20] through a postulated intermediacy of an hydroxylamine species;[24] thus, it is reasonable to assume an incomplete oxidation and the presence of a monoradical hydroxylamine component. This derivative cannot be easily distinguished from the corresponding biradical by, for example, UV−vis spectroscopy. Although UV−vis spectra of C_{60} derivatives have been extensively used for the discrimination between mono- and bisadducts, and among isomeric bisadducts, they cannot be employed to characterize fullerene bisadducts with the same addition pattern but different functionalities. Also mass spectrometry failed to reveal the mentioned impurity, whose molecular mass coincides with that of the ^{13}C-containing biradical.

After allowing for the presence of the monoradical component, the overall agreement with experimental data was found to be rather good. The overall procedure was proven to be very stable, and the full set of parameters (D_x, D_y, D_z, and J; distance R and weight p) described in the previous section was fitted together, i.e., in a single search. In all cases convergence to a unique set of optimized parameters required less than 100 spectrum evaluations, indicating the existence of a relatively sharp region of validity of the model in the parameter space; in

(22) Vasavada, K. V.; Schneider, D. J.; Freed, J. H. *J. Chem. Phys.* **1987**, *86*, 647.
(23) Mazzoni, M.; Franco, L.; Ferrarini, A.; Corvaja, C.; Zordan, G.; Scorrano, G.; Maggini, M. *Liquid Crystals* **2002**, *29*, 203−208.
(24) Trahanovsky, W. S. *Oxidation in Organic Chemistry*; Academic Press: New York 1978; p 267 and references therein.

Table 1. Geometrical and Rotational Parameters Obtained for Conformers **1**−**5**[a]

isomer	R/nm	ϕ_1, θ_1	ϕ_2, θ_2	Ω_1	Ω_2	$D_i \times 10^{-9}$/Hz	J/mT	p
1	0.66	0, 0	180, 0	0, 90, 0	180, 90, 0	0.15, 2.5, 4.6	−8.94	0.83
2	0.58	−75, 0	75, 0	75, 45, 90	−75, 45, 90	0.31, 2.0, 2.2	2.29	0.85
3	0.61	−60, 0	60, 0	90, 72, 90	90, 60, −45	0.93, 0.95, 0.1	−1.70	0.84
4	0.66	−50, 0	50, 0	120, 135, 90	60, 55, 90	0.66, 4.9, 0.98	0.95	0.73
5	0.73	−45, 0	45, 0	−90, 135, 0	0, 90, −45	0.04, 1.0, 1.6	30.5	0.85

[a] All angles are expressed in degrees.

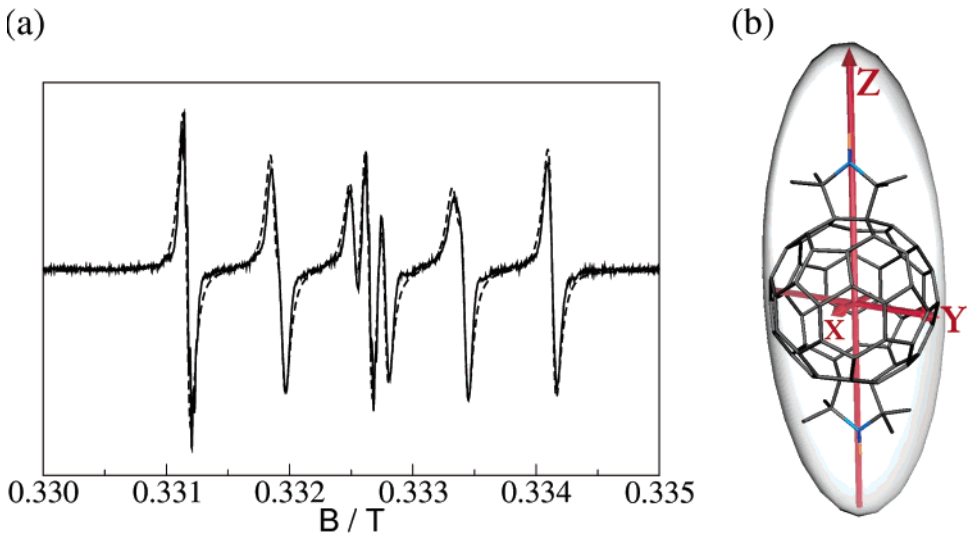

Figure 3. (a) Experimental (full line) and simulated (dashed line) ESR spectrum of isomer **1**; (b) principal axis of diffusion tensor of isomer **1**.

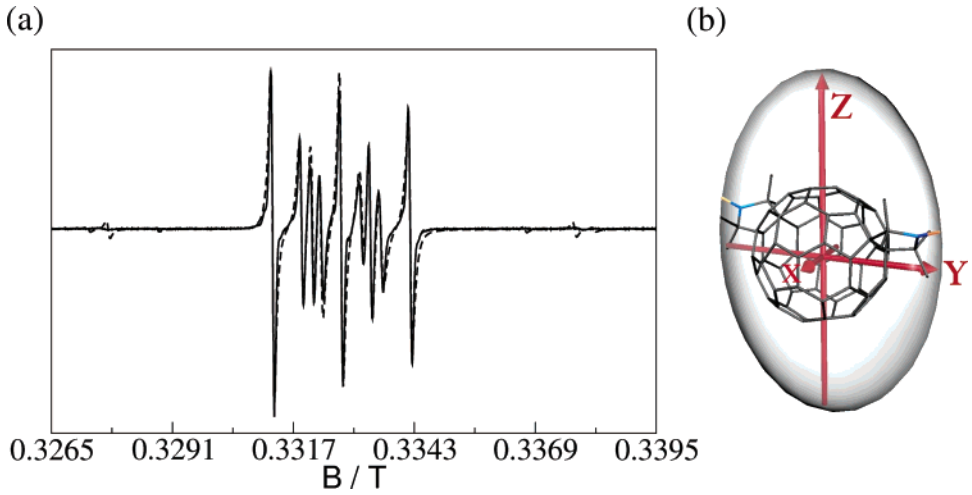

Figure 4. (a) Experimental (full line) and simulated (dashed line) ESR spectrum of isomer **2**; (b) principal axis of diffusion tensor of isomer **2**.

other words, the model is sensitive in its discrimination of structural changes. This is in fact due to several reasons. (*i*) The five isomers present very different values of the constant J, and four of these values fall in a region where even small changes of J involve appreciable changes in the spectrum shape; one therefore expects and finds relatively sharp minima with respect to the J parameter. (*ii*) Initial values employed in the fitting for distance R are based on good estimates coming from molecular mechanics calculations of the overall geometry of each conformer (see below). (*iii*) Finally, the only effect of p on the spectrum is related to the intensity of the three principal lines, having no effect on their position or width. In this way, three of the six parameters (J, R, and p) are limited to vary within a restricted range of values which is characteristic of each conformer.

Results are summarized in Table 1 and in Figures 3−7, in which the simulated and experimental spectra are accompanied by the molecular geometry to which an ellipsoid is superimposed, representing the principal values of diffusion tensor and the directions of principal axes of MF.

As an exercise, a comparison has also been made between values of the nitroxide−nitroxide distance, obtained from fitting the experimental ESR spectra, and estimates of the same quantities obtained by a standard molecular mechanics (MM) program.[25] The values reported in Table 2 are in accord within 10% with the inter-radical distance taken from the midpoints of the NO bonds. This is an approximation based on the consideration that in nitroxide the spin density is equally

(25) Tinker Molecular Modeling homepage, http://dasher.wustl.edu/tinker/.

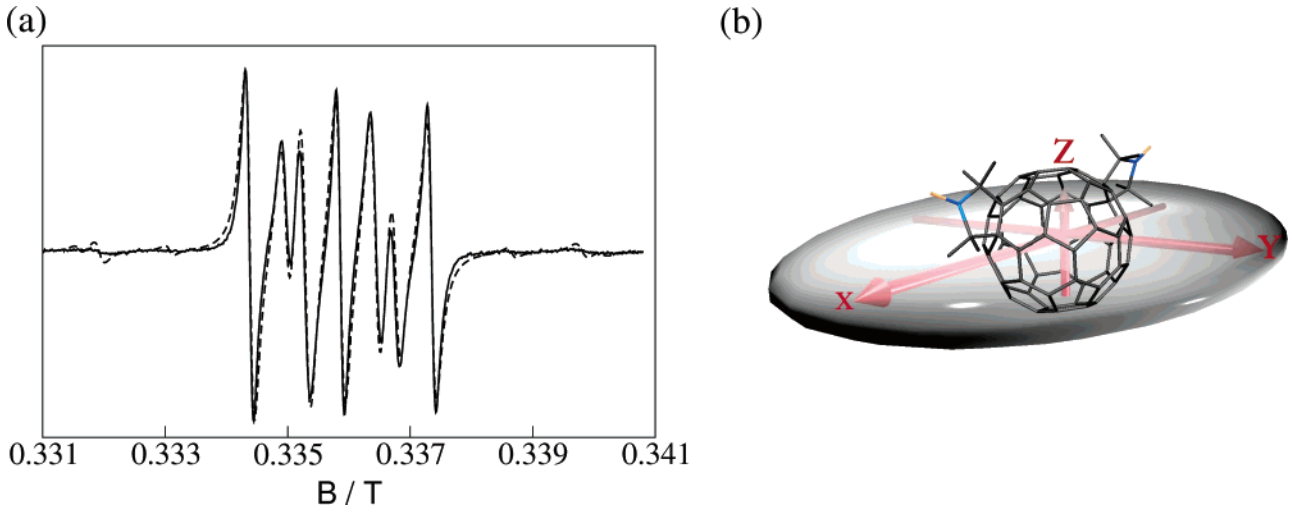

Figure 5. (a) Experimental (full line) and simulated (dashed line) ESR spectrum of isomer **3**; (b) principal axis of diffusion tensor of isomer **3**.

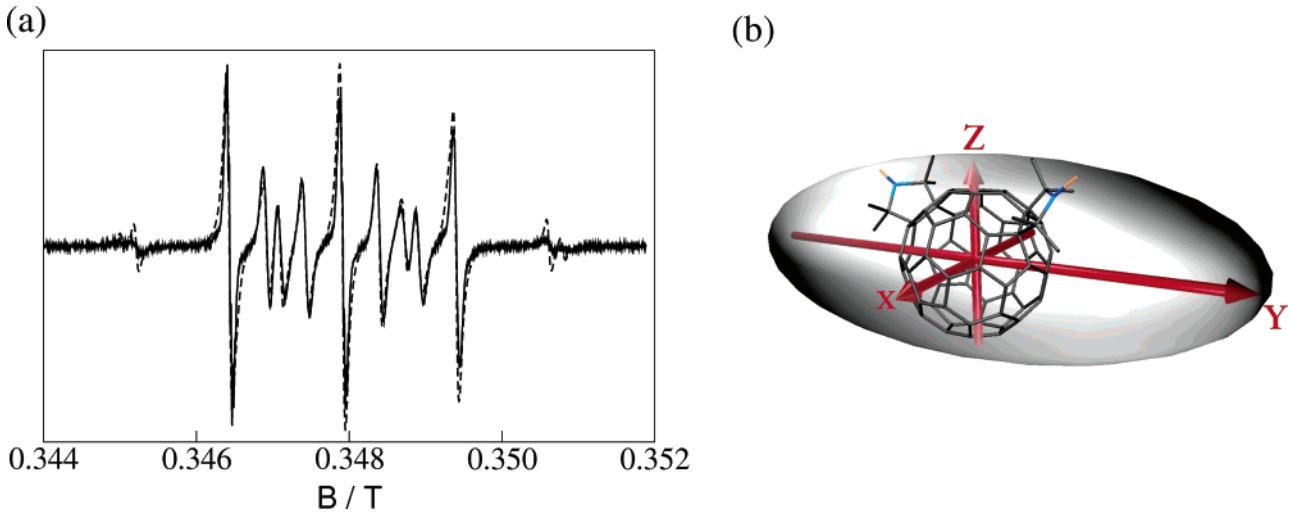

Figure 6. (a) Experimental (full line) and simulated (dashed line) ESR spectrum of isomer **4**; (b) principal axis of diffusion tensor of isomer **4**.

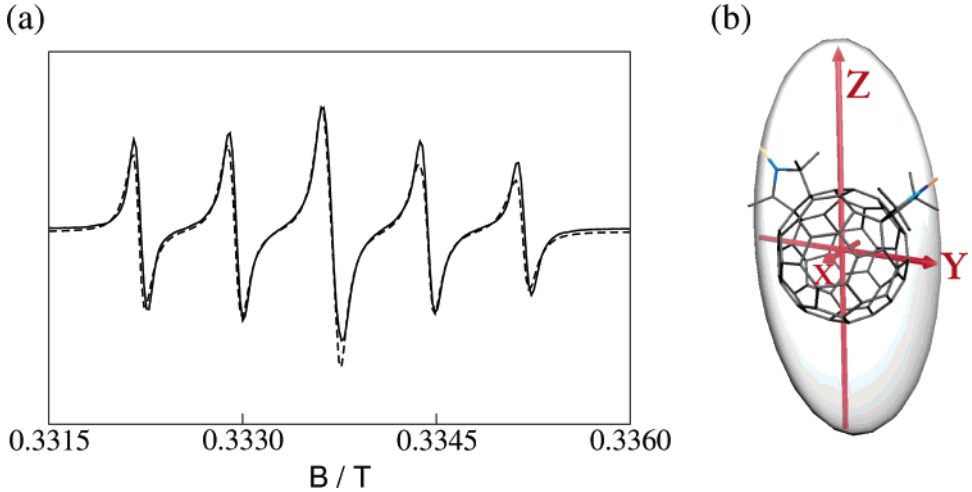

Figure 7. (a) Experimental (full line) and simulated (dashed line) ESR spectrum of isomer **4**; (b) principal axis of diffusion tensor of isomer **5**.

distributed between the nitrogen and the oxygen atoms.[26] The rather good overall agreement of the model with experiments is best seen in Figures 3−7, where the experimental spectra of the biradicals **1**−**5** are shown together with the best fit spectra. Some small discrepancies in the line shape are present in the case of **2** (see Figure 4) for which a spectrum with very narrow lines has been recorded, showing additional small splittings

(26) (a) Miller, J. S.; Epstein, A. J. *Angew. Chem., Int. Ed. Engl.* **1994**, *33*, 385. (b) Brown, P. J.; Capiomont, A.; Gillon, B.; Schweizer, J. *J. Magn. Magn. Mater.* **1979**, *14*, 289.

Table 2. Comparison between Probe−Probe Distances Estimated by Fitting SLE Simulated Spectra to Experimental One (r_{fit}) and Obtained by Standard Molecular Mechanics Calculation (r_{NN} = Nitrogen−Nitrogen Distance, r_{OO} = Oxygen−Oxygen Distance, Obtained by Tinker MM Program)

isomer	r_{NN}/Å	r_{OO}/Å	$(r_{NN} + r_{OO})/2$/Å	r_{fit}/Å	% error[a]
1	12.03	14.30	13.16	13.12	−0.3
2	11.65	14.04	12.84	11.31	−11.9
3	10.24	12.02	11.13	10.77	−3.2
4	9.72	11.57	10.64	10.34	−2.8
5	8.74	10.72	9.73	10.33	+6.2

[a] Percentage errors are given to compare fitted values and calculated $(r_{NN} + r_{OO})/2$.

caused by the hyperfine interaction of the methyl protons. For the other biradicals these splittings are unresolved but contribute to the line shapes, giving them a Gaussian contribution. ^{13}C satellites appearing in some of the spectra, particularly evident in those of isomers **1** and **2**, are not reproduced, since they are not included in the model. Moreover, the width of the small intensity lines due to singlet-to-triplet transitions[15] occurring in the wings region of the spectra (see Figures 5 and 6) is poorly reproduced, but their position is properly obtained. This is not unexpected since these lines are severely affected by small-amplitude modulation of *J* interaction, which also is not included in the model.[15] The positive sign of *J* of the isomer **5** (equatorial) and the negative sign of isomer **1** (*trans*-**1**) agree with what is expected on simple considerations.[20] The exchange interaction is ferromagnetic when the unpaired electron wave functions are orthogonal to each other and antiferromagnetic when they overlap. Magnitudes of *J* and their dependence upon distance for these systems were tentatively rationalized previously.[20] Systematic quantum mechanics calculations should be carried out, but they are outside the aim of this work.

CW-ESR spectrum shape is severely affected by the magnitude of *J*. To provide didactic illustration of the model flexibility, we have calculated a series of spectra for isomer **1**, maintaining constant all the magnetic and geometric parameters as obtained by the best fit, and varying the exchange interaction *J*.

In Figure 8, we show the progression of simulated spectra obtained for decreasing values of the adimensional ratio *J*/*a* (where *a* is the trace of the **A** tensors) which takes the value of −5.387 in the experimental-related case. In principle all *J*/*a* ratios can be determined reliably, although the fitting procedure may become uncertain when $|J/a| \gg 1$. In practice, in our case, simulated spectra are essentially independent from variation of $|J/a|$ for $|J/a| > 50$.

IV. Conclusions

In this work, our main goal has been to show the potential usefulness of the stochastic Liouville approach in dealing with multiprobe systems by starting to analyze relative well-known, clearly defined chemical model systems. Our results are encouraging, since structural, energetic, and dynamic parameters are promptly obtained by the SLE approach. Structural parameters are directly recovered in the form of inter-radical distances. Energy parameters, namely the exchange interaction constant *J*, are also evaluated. The fitted parameters include the exchange interaction constant *J with its sign*. The simulated spectrum sensitivity to the sign of *J* is shown in Figure 9. For all the examined derivatives, the resulting signs coincide with those obtained by ENDOR spectroscopy.[20] This is worth pointing out

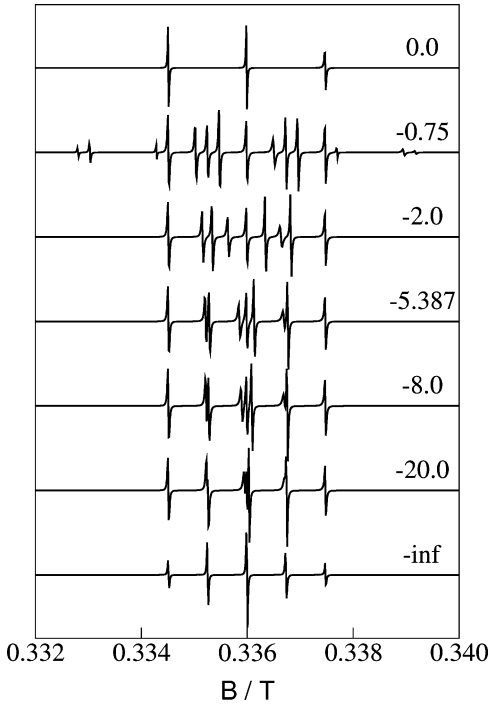

Figure 8. Variation of calculated ESR spectra (molecular geometry of isomer **1)** with respect to ratio *J*/*a*.

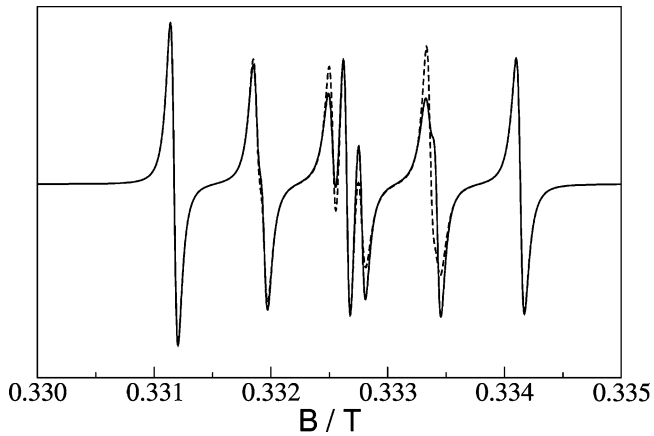

Figure 9. Variation of calculated ESR spectra with respect to the sign of *J*. Parameters for isomer **1** are considered, solid line ($J/a = -5.387$); opposite *J* sign, dashed line ($J/a = +5.387$).

since the sign of *J* does not influence the ESR line positions and its determination is not straightforward. However, for structural information it is important to take the sign into proper consideration, and any way to determine it is welcome, because the ENDOR technique is not always applicable. Finally, reasonable estimates of dynamic parameters, such as the rotation diffusion tensors, are directly obtained by the SLE solution, which is in accordance with the known molecular structure. Figure 10 shows the effect of altering the diffusion tensor values on the spectrum, moving away from the optimal set of parameters.

The nice agreement between experimental and calculated spectra, verified for all biradicals in the examined series, confirms the idea that the described methodology can be applied with good confidence for investigating structural and dynamic properties of more complex systems, such as doubly labeled peptides and biopolymers. Of course, for such cases the model

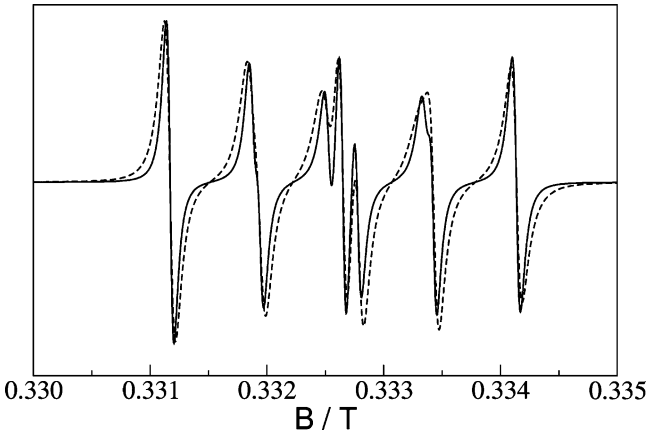

Figure 10. Variation of calculated ESR spectra with respect to diffusion. Parameters for isomer **1** are considered, solid line (values of D_i reported in Table 1); one-third of the values of D_i, dashed line.

should be extended and modified. For a start, in the case of rigid systems of unknown structure, the necessary straightforward improvement consists of the inclusion among the fitting parameters of the angles specifying the nitroxide orientation relative to the diffusion tensor. For flexible systems the internal motions should be also explicitly considered. Work in this direction will require a careful definition of primary relaxation processes, i.e., motional contributions to the SLE, based on many-body stochastic formalism (e.g. N-body diffusive operators to allow the description of lateral and backbone motions).

Acknowledgment. This work was supported by MIUR (Grants FIRB RBNE01P4JF, FIRB RBAU017S8R and PRIN 2004035502).

Supporting Information Available: Examples of ESR experimental (solid lines) and simulated (dashed lines) spectra for the biradical isomer **2**. This material is available free of charge via the Internet at http://pubs.acs.org.

JA057414I